X International Conference on Computational Methods in Marine Engineering
MARINE 2023
J. García-Espinosa, L. González, J.E. Gutiérrez & B. Serván-Camas (Eds)

Moving Contact Line and No-Slip Boundary Conditions for High-Speed Planing Hulls

Zhaoyuan Wang and Frederick Stern*

IIHR-Hydroscience & Engineering, University of Iowa, Iowa City, IA 52242, USA, web page: https://www.iihr.uiowa.edu//

* Corresponding author: Frederick Stern, frederick-stern@uiowa.edu

ABSTRACT

In this study, the classical "moving-contact-line" problem associated with the no-slip boundary condition (BC) is examined, with a particular focus on large-scale, high Reynolds number turbulent ship flows. Numerical ventilation is one of the main issues reported for the computational prediction of the high-speed small planing craft using the Volume-of-Fluid (VOF) method. A numerical strategy is presented to resolve this issue with a wave blanking distance defined and used when solving the VOF equations, which is chosen based on the y^+ values and the velocity profiles in the boundary layer. A series of numerical tests are conducted using a slamming plate and a high-speed planing step hull. The numerical experiments show that if the blanking distance is $y^+ < 30$ (inside the buffer and viscous sublayers), the air-water interface on the wall will be unstable and numerical ventilation will occur. For the blanking distance $y^+ > 30$ (outside the buffer layer), the air-water contact line is smooth and air entrainment can be avoided. It is suggested that the blank distance needs to satisfy $30.0 < y^+ < 200.0$ in consideration of accuracy and stability, and a value of $y^+ \sim 100.0$ can be used in practice.

Keywords: moving contact line; no-slip; planing hull; numerical ventilation; VOF.

NOMENCLATURE

d_{blank}	Wave blanking distance
Err	Relative error
Fr_b	Beam based Froude number $Fr_b = U_\infty/\sqrt{gb}$
l	Slip length [m]
u^*	Friction velocity [m s^{-1}]
u	Local velocity [m s^{-1}]
y^+	Non-dimensional wall distance $y^+ = \frac{u^* y}{\nu}$
U_∞	Free stream velocity [m s^{-1}]
CFD	Computational Fluid Dynamics
EFD	Experimental Fluid Dynamics

1. INTRODUCTION

The no-slip boundary condition (BC) is usually used at the solid surfaces for the numerical simulation of viscous flows, which assumes that fluid velocity is zero relative to the solid surface. The fluid

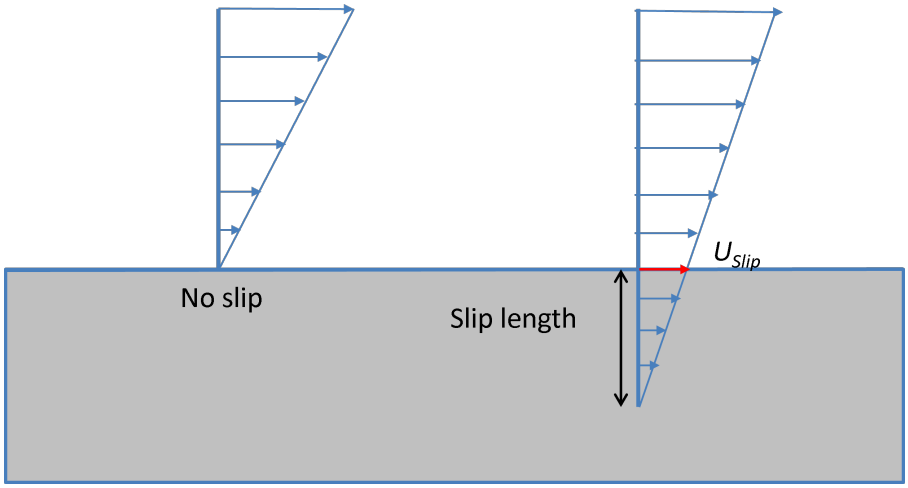

Figure 1: No slip and slip boundary conditions.

particles are stuck on the solid surface rather than move along with the flow. This assumption is accurate and acceptable for most macroscopic fluid flows, but may be invalid and pose problems for microscopic-scale flows. For small scale flows where the mean free path of the fluid is close to the characteristic length (Rothstein, 2010), e.g., flows of rarified gases, gas molecules on the solid surface can move freely. The no-slip BC also fails for viscous flows with a moving contact line. The moving contact line is defined as the interface between two immiscible fluids that intersects with the solid surface. For example, the air-water interface on the ship surface will not move if the no-slip BC is used.

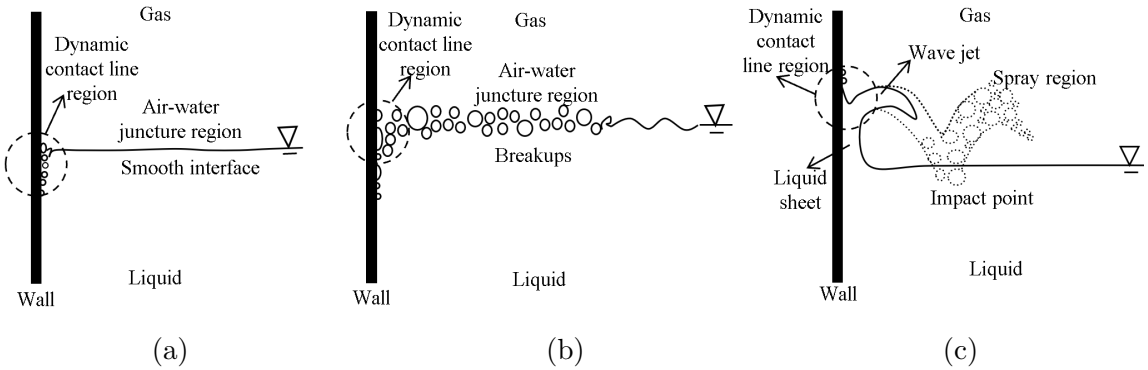

Figure 2: Three possible interface configurations in the liquid-solid-gas juncture regions.

For small scale flows, the slip BC with a finite slip length is usually used as shown in Figure 1. The slip velocity is defined as

$$u_{slip} = l \left| \frac{\partial u}{\partial y} \right|. \tag{1}$$

The contact line movement is also dependent on the contact angles when surface tension force is dominant, but the mechanism is not fully understood. It should be noted that most previous studies have been focused on small scale flows, such as flows within microfluidic or nanofluidic devices, and small bubbles/droplets (Mohammad Karim, 2022; Rothstein, 2010). Few studies have been reported for large scale flows, such as ship flows. For ship flows, the complexity is due to the interactions of the multi-phase turbulent flow with the solid surface in the liquid-solid-gas juncture region. Typical

interface configurations in the juncture region for ship flows are shown in Figure 2, where the air water interface varies from a smooth surface, to breakup, and an overturning liquid sheet depending on different geometries and flow conditions (Longo et al., 1998; Metcalf et al., 2006; Sreedhar and Stern, 1998; Wang et al., 2012; Waniewski et al., 2002). The Reynolds numbers are usually high and very small grid spacing is needed near the wall to resolve the boundary layer, where the numerical treatments used for the small-scale flows are not suitable. One of the issues caused by the no-slip BC is the numerical ventilation (Cucinotta et al., 2021), which is especially serious for CFD predictions of high-speed small planing craft using the algebraic volume-of-fluid (VOF) method for air-water interface modeling. VOF slip velocity is used by Wheeler et al. (2021) to minimize the numerical ventilation effect.

In the present study, a numerical strategy to handle the no-slip BC and moving contact line problem for high-speed planing hulls is proposed. A blanking distance from the solid surface is used when solving the interface modeling equations, which is chosen based on the y^+ values and the velocity profiles in the boundary layer. A series of numerical tests are conducted using a slamming plate and a high-speed planing step hull. The numerical experiments show that if the blanking distance is $y^+ < 30$ (inside the buffer and viscous sublayers), the air-water interface on the wall will be unstable and numerical ventilation will occur. For the blanking distance $y^+ > 30$ (outside the buffer layer), a smooth air-water contact line can be obtained without air entrainment. It is suggested that the blanking distance needs to satisfy $30.0 < y^+ < 200.0$ in consideration of accuracy and stability, and a value of $y^+ \sim 100.0$ can be used in practice.

The numerical methods used in the present study will be given in the next section including the interface modeling method and definition of the wave blanking distance. The numerical tests of a vertical slamming plate and application example of a step planing hull will be presented in Section 3, followed by the conclusion in the last section.

2. NO-SLIP WALL BOUNDARY CONDITIONS AND MOVING CONTACT LINE

2.1 No-slip Wall Boundary Conditions

As mentioned in the previous section, high Reynolds number multi-phase turbulent flows are involved in ship flows. For the numerical simulations, no-slip wall BC with proper turbulence models (e.g., RANS) and very small grid spacing ($y^+ \sim 1$) near the surface of the hull are needed in order to resolve the boundary layer. It should be noted that numerical ventilation usually does not cause serious problems for the CFD prediction of displacement hulls using the no-slip wall BC with moving contact lines. Unlike displacement hulls, however, the wetted area of planing hulls can change abruptly and significantly due to slamming, and the size of which is also comparable to the jets and sprays generated. Special numerical treatment is needed to handle the no-slip BC and moving contact line problem for high-speed planing hulls, which is critical for the correct prediction of jets, sprays, wave breaking, and ventilation near and around hulls, and their effects on forces and ship motions.

2.2 Moving Contact Line

In the present study, the geometric VOF method (Wang et al., 2012) is used for the interface modeling with a distance function for the interface representation. The distance function is obtained directly from the reconstructed interface. A distinct and sharp air-water interface can be precisely defined, which differs from the smeared air-water interface usually obtained using the algebraic VOF method. An example of the velocity profile near the wall using the no-slip BC is shown in Figure 3. It is clear

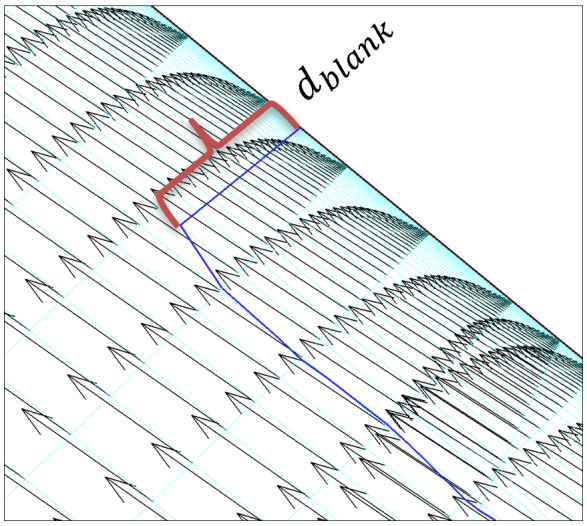

Figure 3: Velocity profile and wave blanking for the free surface flow in CFDShip-Iowa.

that the fluid particles near the wall move at a slower speed than those away from it. Air entrainment will occur when an air-water interface is present, ultimately leading to numerical ventilation. Herein, a wave blanking distance, d_{blank}, will be used when solving the VOF interface equations. The d_{blank} is defined as the distance in the normal direction of the wall (see Figure 3). The VOF interface equations will not be solved if the the computational cells are located within the blanking distance and the values of the VOF and distance functions in these cells will be extrapolated from the cells outside of the blanking region. The d_{blank} will be chosen based on the y^+ values and the velocity profiles in the boundary layer. In the following section, numerical experiments will be conducted with different d_{blank} values and proper wave blanking value will be recommended.

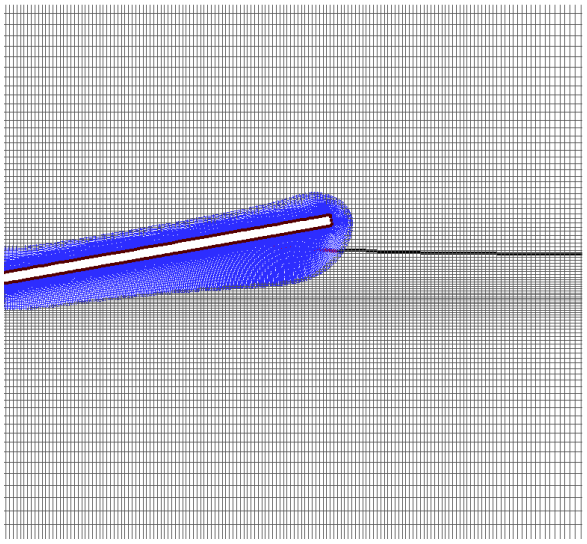

Figure 4: Grids of a flat plate slamming onto a water surface.

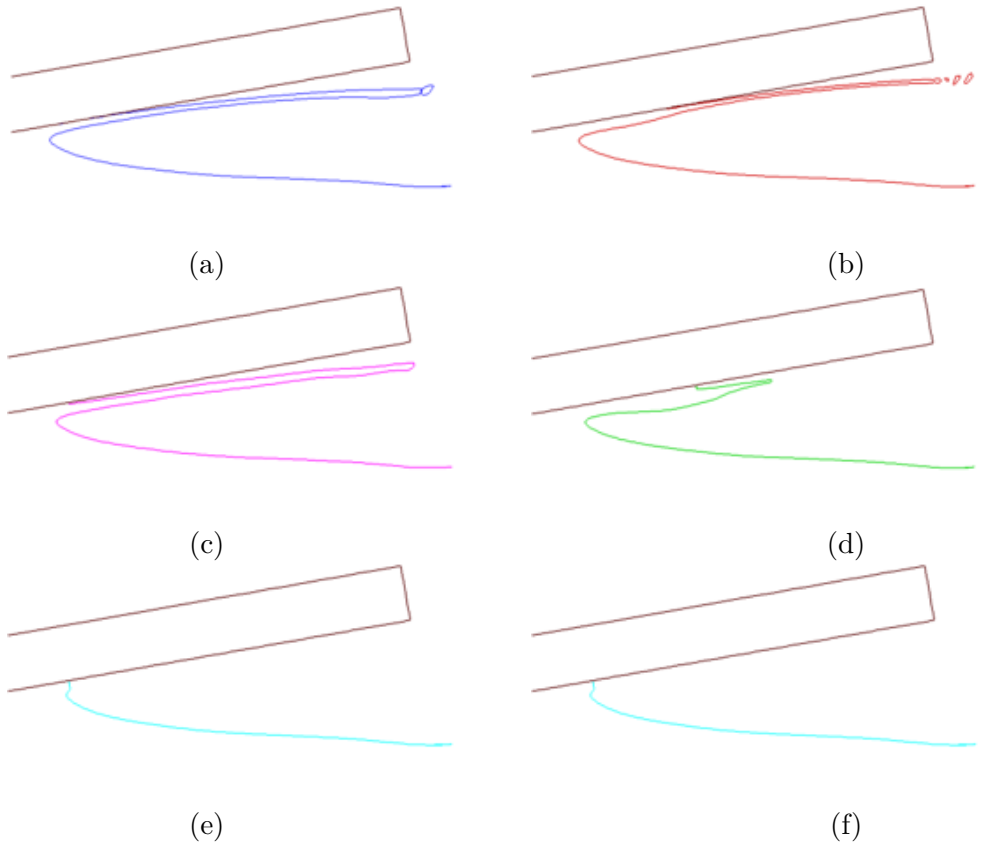

Figure 5: Vertical slamming plate test. (a) $d_{blank} = 0.6 \times 10^{-4}$ ($y^+ = 1.0$); (b) $d_{blank} = 1.0 \times 10^{-4}$ ($y^+ = 3.5$); (c) $d_{blank} = 3.0 \times 10^{-4}$ ($y^+ = 10.0$); (d) $d_{blank} = 9.0 \times 10^{-4}$ ($y^+ = 30.0$); (e) $d_{blank} = 2.0 \times 10^{-3}$ ($y^+ = 67.0$); (f) $d_{blank} = 3.0 \times 10^{-3}$ ($y^+ = 100.0$).

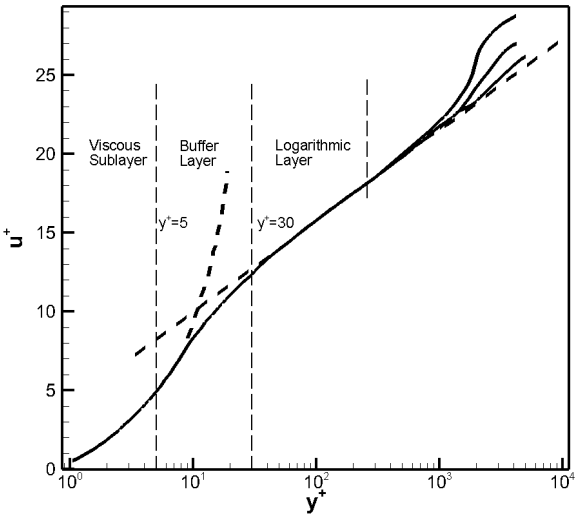

Figure 6: Boundary layer velocity profile.

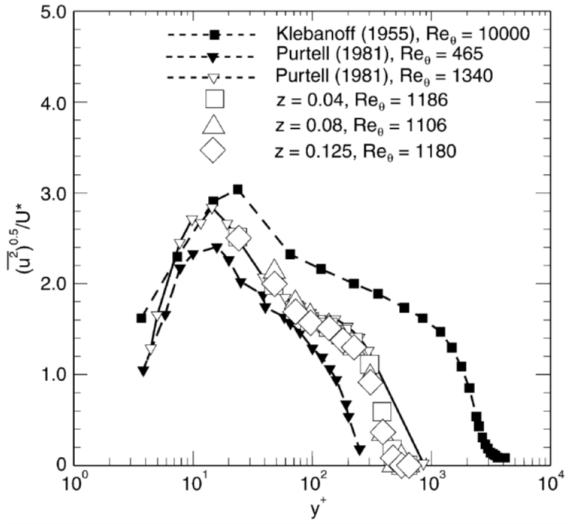

Figure 7: Stream-wise normal Reynolds stress near a surface-piercing flat plate (Longo et al., 1998).

3. NUMERICAL TESTS AND APPLICATION EXAMPLES

In this section, the wave blanking distance is applied to the VOF equations using the structured grid flow solver, CFDShip-Iowa V5.5 (Wang and Stern, 2022). CFDShip-Iowa V5.5 is a multi-phase flow solver developed based on the single-phase flow solver, CFDShip-Iowa V4.5 (Huang et al., 2008), for ship flows involving complex phenomena such as wave breaking, air entrainment, spray, and mixed cavitation/ventilation. The functionalities of the code include six degrees of freedom (6DOF) motions with dynamic overset grids, turbulence, moving control surfaces, multi-objects, advanced controllers, propulsion models, incoming waves and winds, bubbly flow, and fluid-structure interaction. The overset grid package SUGGAR (Noack, 2005) is used for computing the domain connectivity information between overlapping grids. Details of the mathematical models and numerical methods can be found in the above papers and references therein.

3.1 Numerical Tests

The impact of a flat plate onto a water surface is simulated on a two-dimensional domain with two block overset grids as shown in Figure 4. A deadrise angle of 10° and a pitch angle of 0° are considered for the slamming with a Froude number of $Fr = 0.42$. Details of the geometry and setup can be found in the study by Pellegrini et al. (2020).

Figure 5 shows the comparison of the air-water interface underneath the plate with various wave blanking distances including the corresponding y^+ values. As shown in the figure, very thin water jets are created under the plate for small blanking distances with $y^+ < 30$. This is because the interface on the wall does not move or moves much slower than that away from the wall. Air can be entrapped under the plate when the jet breaks up, which is different from the experimental observations. The nonphysical air entrainment will affect the accuracy of the force calculations and computational stability. For the large blanking distances with $y^+ > 30$, water jet is not formed and the contact line is smooth, especially for $y^+ > 100$.

It should be noted that the wave blanking distances chosen based on the y^+ values correspond to different regions of the wall boundary layer velocity distribution as shown in Figure 6. If the wave

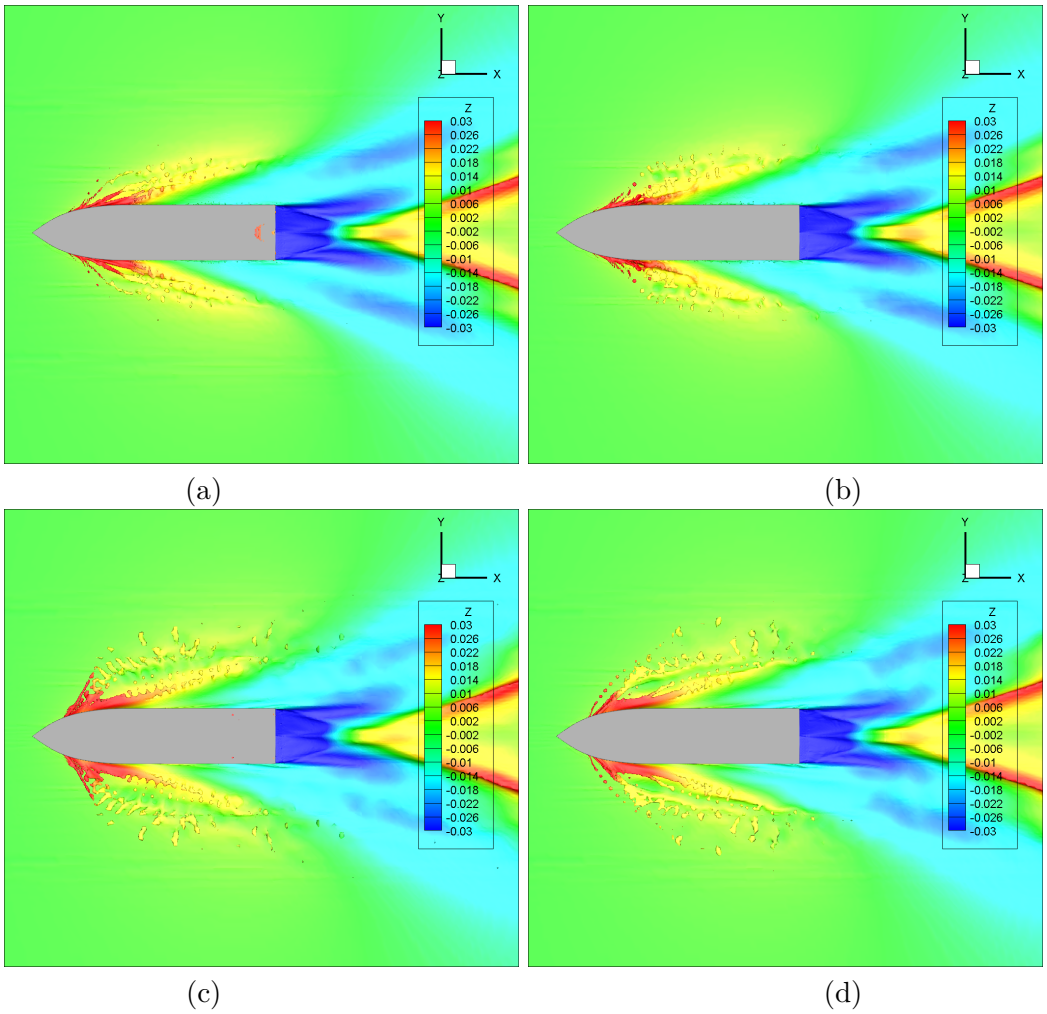

Figure 8: Top view of the wave profiles of a single step planing hull. (a) $d_{blank} = 2.0 \times 10^{-4}$ ($y^+ = 46.0$); (b) $d_{blank} = 3.0 \times 10^{-4}$ ($y^+ = 68$); (c) $d_{blank} = 5.0 \times 10^{-4}$ ($y^+ = 113.0$); (d) $d_{blank} = 1.0 \times 10^{-3}$ ($y^+ = 228.0$).

blanking distance is inside the buffer layer and viscous sub-layer regions, non-smooth contact line with a very thin water jet and non-physical ventilation will occur. The flows within these layers are not stable and very large Reynolds stress can be observed as shown in Figure 7 for a surfacing-piercing flat plate. Therefore, the blanking distance should be chosen outside of the buffer layer with $y^+ > 30$ for a smooth air-water interface and to avoid nonphysical ventilation.

3.2 Application Examples

A single step planing craft is chosen for the simulations to study the wave blanking effect on the wave profiles, forces, and motions. The Found number is $Fr_b = 1.463$. 2DoF motions of heave and pitch are considered using the dynamic overset grid. Details of the geometry, grids, and computational setup can be found in the study by Park et al. (2022). Note that all the wave blanking distances used herein are outside of the buffer layer with $y^+ > 30$.

Figure 8 shows top view of the wave profiles computed with different wave blanking distances. The bottom view of the wave profiles with ventilated step region is shown in Figure 9 including the

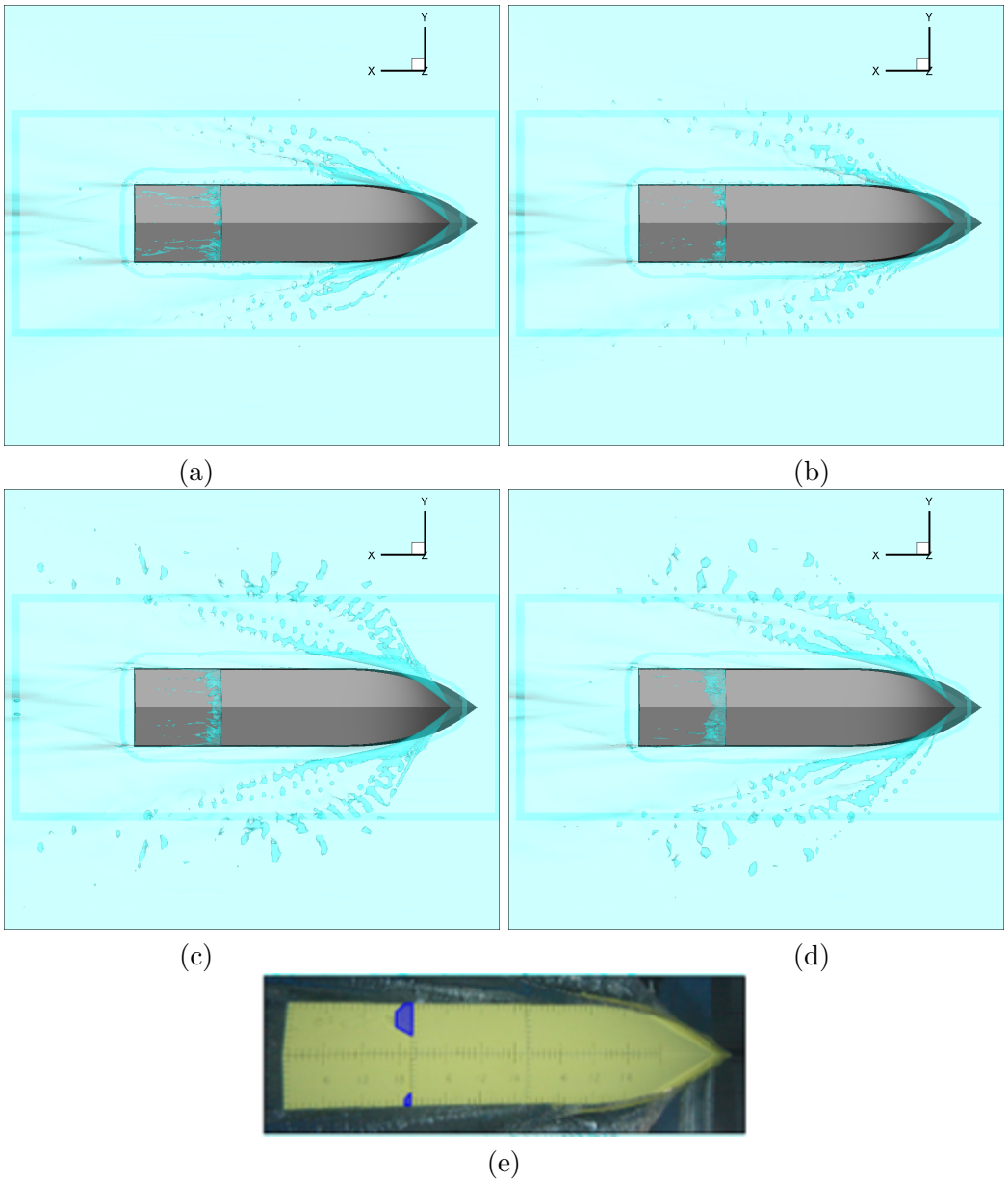

Figure 9: Bottom view of the wave profiles of a single step planing hull. (a) $d_{blank} = 2.0 \times 10^{-4}$ ($y^+ = 46.0$); (b) $d_{blank} = 3.0 \times 10^{-4}$ ($y^+ = 68$); (c) $d_{blank} = 5.0 \times 10^{-4}$ ($y^+ = 113.0$); (d) $d_{blank} = 1.0 \times 10^{-3}$ ($y^+ = 228.0$). (e) Experimental image.

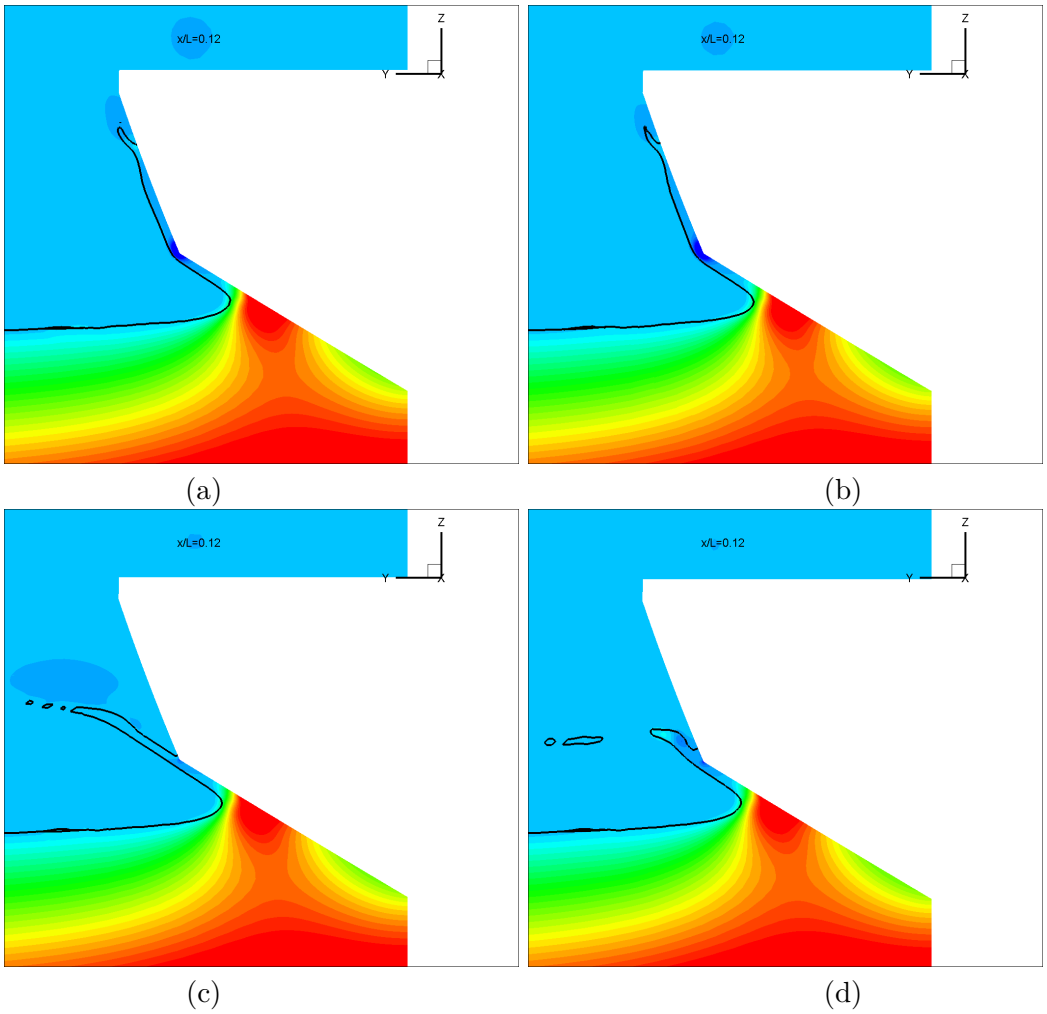

Figure 10: Wave profiles and pressure distribution on the cross section of a single step planing hull. (a) $d_{blank} = 2.0 \times 10^{-4}$ ($y^+ = 46.0$); (b) $d_{blank} = 3.0 \times 10^{-4}$ ($y^+ = 68$); (c) $d_{blank} = 5.0 \times 10^{-4}$ ($y^+ = 113.0$); (d) $d_{blank} = 1.0 \times 10^{-3}$ ($y^+ = 228.0$).

experimental image. As shown in the figures, the wave spread increases with the wave blanking distance. The air ventilation region under the step of the hull also increases with the wave blanking distance. Generally, the size of the ventilation region is comparable to the experimental observation. The slices of the wave profile and pressure distribution cut in the stream-wise direction are shown in Figure 10. The figure shows that the water jet separates from the hull with the increase of the wave blanking distance. For a small wave blanking distance, a water film is formed and stuck on the hull. The computation using a large wave blanking distance is more stable as compared to that using a small one. The comparison of forces and motions is shown in Table 1. Generally, both forces and motions improved with the decrease of the wave blanking values. The results are comparable for cases with $y^+ < 100$. Therefore, the wave blanking distance with $30 < y^+ < 200$ should be used in consideration of accuracy and stability, and a value of $y^+ \sim 100$ can be used in practice.

Table 1: Comparison of the force and motions for a singe step hull at Fr_b=1.463.

	Force (N)	Err(%)	Heave (mm)	Err(%)	Pitch(deg)	Err(%)
EFD	49.469		0.445		4.216	
$y^+ = 228$	47.69	3.596	4.336	874.4	3.542	15.99
$y^+ = 113$	48.51	1.938	4.305	867.4	3.589	14.87
$y^+ = 68$	48.32	2.322	3.889	754.7	3.725	11.64
$y^+ = 46$	48.58	1.797	4.065	793.4	3.723	11.69

4. CONCLUSIONS

The no-slip BC is usually used at the solid surfaces for numerical simulations of viscous flows, which is accurate for most macroscopic flows but invalid when a moving contact line is present. This problem is examined in the present study with a particular focus on large-scale, high Reynolds number turbulent ship flows. A numerical strategy is proposed to resolve the no-slip BC and moving contact line problem for high-speed planing hulls. A wave blanking distance is defined and used to solve the VOF based interface modeling equations, which is chosen based on the y^+ values and the velocity profiles in the boundary layer.

Numerical tests and application examples are performed using a vertical slamming plate and a high-speed planing step hull. The numerical results of the slamming plate show that if the blanking distance is $y^+ < 30$ and falls within the buffer and viscous sublayers, the air-water interface on the wall will be unstable and numerical ventilation will occur. For the blanking distance $y^+ > 30$ and outside the buffer layer, a smooth air-water contact line can be obtained without air entrainment. The computational results of the planing step hull show that both forces and motions are improved with the decrease of the wave blanking value. The results are comparable for cases with $y^+ < 100$. The computation using a large wave blanking distance is more stable than that using a small wave blanking. Therefore, it is suggested that the blanking distance needs to satisfy $30.0 < y^+ < 200.0$ in consideration of accuracy and stability, and a value of $y^+ \sim 100.0$ can be used in practice.

ACKNOWLEDGEMENTS

This work is supported by the Office of Naval Research grants N00014-20-1-2259 and N00014-22-1-2413 under the administration of Dr. Robert Brizzolara. The simulations presented in this work were performed at the Department of Defense (DoD) Supercomputing Resource Centers (DSRCs) through the High Performance Computing Modernization Program (HPCMP).

AUTHOR'S CONTRIBUTION

ZW conducted the numerical tests and simulation, processed the data, and wrote the first draft of the manuscript. FS supervised and coordinated the project. Both authors edited and approved the manuscript.

REFERENCES

Cucinotta, F., Mancini, D., Sfravara, F., & Tamburrino, F. (2021). The effect of longitudinal rails on an air cavity stepped planing hull. *Journal of Marine Science and Engineering*, *9*(5).

Huang, J., Carrica, P. M., & Stern, F. (2008). Semi-coupled air/water immersed boundary approach for curvilinear dynamic overset grids with application to ship hydrodynamics. *International Journal for Numerical Methods in Fluids*, *58*(6), 591–624.

Longo, J., Huang, H. P., & Stern, F. (1998). Solid/free-surface juncture boundary layer and wake. *Experiments in Fluids*, *25*(4), 283–297.

Metcalf, B., Longo, J., Ghosh, S., & Stern, F. (2006). Unsteady free-surface wave-induced boundary-layer separation for a surface-piercing NACA 0024 foil: Towing tank experiments. *Journal of Fluids and Structures*, *22*(1), 77–98.

Mohammad Karim, A. (2022). A review of physics of moving contact line dynamics models and its applications in interfacial science. *Journal of Applied Physics*, *132*(8), 080701.

Noack, R. (2005). SUGGAR: A general capability for moving body overset grid assembly. *AIAA paper 2005-5117*.

Park, S., Wang, Z., Stern, F., Husser, N., Brizzolara, S., Morabito, M., & Lee, E. (2022). Single- and two-phase cfd v&v for high-speed stepped planing hulls. *Ocean Engineering*, *261*, 112047.

Pellegrini, R., Diez, M., Wang, Z., Stern, F., Wang, A., Wong, Z., Yu, M., Kiger, K., & Duncan, J. High-fidelity FSI simulations and v&v of vertical and oblique flexible plate slamming. In: In *33rd symposium on naval hydrodynamics*. Osaka, Japan, 2020, October.

Rothstein, J. P. (2010). Slip on superhydrophobic surfaces. *Annual Review of Fluid Mechanics*, *42*(1), 89–109.

Sreedhar, M., & Stern, F. (1998). Large eddy simulation of temporally developing juncture flows. *International Journal for Numerical Methods in Fluids*, *28*(1), 47–72.

Wang, Z., & Stern, F. (2022). Volume-of-fluid based two-phase flow methods on structured multiblock and overset grids. *International Journal for Numerical Methods in Fluids*, *94*(6), 557–582.

Wang, Z., Yang, J., & Stern, F. (2012). A new volume-of-fluid method with a constructed distance function on general structured grids. *Journal of Computational Physics*, *231*(9), 3703–3722.

Waniewski, T., Brennen, C., & Raichlen, F. (2002). Bow wave dynamics. *Journal of Ship Research*, *46*.

Wheeler, M. P., Ryan, P., Cimolin, F., Gunderson, A., & Scherer, J. Using vof slip velocity to improve productivity of planing hull cfd simulations. In: In *Sname international conference on fast sea transportation*. OnePetro. Providence, Rhode Island, USA, 2021, October.